A Novel Near-IR Absorbing Ruthenium(II) Complex as Photosensitizer for Photodynamic Therapy and its Cetuximab Bioconjugates

Marta Martínez-Alonso, Albert Gandioso, Chloé Thibaudeau, Xue Qin, Philippe Arnoux, Nurikamal Demeubayeva, Vincent Guérineau, Céline Frochot, Alain Jung, Christian Gaiddon, et al.

A Novel Near-IR Absorbing Ruthenium(II) Complex as Photosensitizer for Photodynamic Therapy and its Cetuximab Bioconjugates

Dr. Marta Martínez-Alonso,[1] Dr. Albert Gandioso,[1#] Chloé Thibaudeau,[2, 3#] Xue Qin,[2,3] Philippe Arnoux,[4] Nurikamal Demeubayeva,[4] Vincent Guérineau,[5] Dr. Céline Frochot,[4] Dr. Alain C. Jung,[2,3]* Dr. Christian Gaiddon,[3,]* and Prof. Dr. Gilles Gasser[1,]*

[1] Chimie ParisTech, PSL University, CNRS, Institute of Chemistry for Life and Health Sciences, Laboratory for Inorganic Chemical Biology, 75005 Paris, France.

[2] Laboratoire de Biologie Tumorale, Institut de cancérologie Strasbourg Europe, 67200 Strasbourg, France.

[3] Université de Strasbourg-Inserm, UMR_S 1113 IRFAC, Laboratory « Streinth », 67200 Strasbourg, France.

[4] Reactions and Chemical Engineering Laboratory, Université de Lorraine, LRGP-CNRS, Nancy, F-54000, France.

[5] Université Paris-Saclay, CNRS, Institut de Chimie des Substances Naturelles, UPR 2301, 91198, Gif-sur-Yvette, France.

[#] These authors have contributed equally to the work.

* Corresponding authors:

E-mail: gilles.gasser@chimeparistech.psl.eu; WWW: www.gassergroup.com; Phone: +33 1 44 27 56 02;

E-mail: gaiddon@unistra.fr

E-mail: a.jung@icans.eu

Abstract

A novel Ru(II) cyclometalated photosensitizer (PS), **Ru-NH$_2$**, for photodynamic therapy (PDT) of formula [Ru(appy)(bphen)$_2$]PF$_6$ (where appy = 4-amino-2-phenylpyridine and bphen = bathophenanthroline) and its cetuximab (CTX) bioconjugates, **Ru-Mal-CTX** and **Ru-BAA-CTX** (where Mal = maleimide and BAA = benzoylacrylic acid) were synthesised and characterised. The photophysical properties of **Ru-NH$_2$** revealed absorption maxima around 580 nm with an absorption up to 725 nm. The generation of singlet oxygen ($^1O_2$) upon light irradiation was confirmed with a $^1O_2$ quantum yield of 0.19 in acetonitrile. Preliminary *in vitro* experiments revealed the **Ru-NH$_2$** was nontoxic in the dark in CT-26 and SQ20B cell lines but showed outstanding phototoxicity when irradiated, reaching interesting phototoxicity indexes (PI) > 370 at 670 nm, and > 150 at 740 nm for CT-26 cells and > 50 with NIR light in SQ20B cells. The antibody CTX was successfully attached to the complexes in view of the selective delivery of the PS to cancer cells. Up to four ruthenium fragments were anchored to the antibody (Ab), as confirmed by MALDI-TOF mass spectrometry. Nonetheless, the bioconjugates were not as photoactive as the **Ru-NH$_2$** complex.

Introduction

Currently approved anticancer metal-based drugs are mainly based on platinum. However, these complexes usually lack selectivity and cause harmful side effects. In order to tackle these drawbacks, other therapeutic modalities, as well as other types of transition metal complexes, have been investigated. Photodynamic Therapy (PDT) is an approved medical technique based on the combined action of a photosensitizer (PS), molecular oxygen, and light. The PS is biologically harmless in the dark but becomes active upon light irradiation thanks, among others, to the formation of singlet oxygen ($^1O_2$), a strong oxidizing agent able to cause cell death.[1] Recently, a Ru(II) polypyridyl complex from the McFarland group (TLD-1433)[2,3] has entered into phase II clinical trials as a new PS for the treatment of a certain form of bladder cancer.[4] Conti and co-workers have recently reviewed the Ru(II) polypyridyl complexes as PS for PDT.[5] One of the aims of a PDT PS is to absorb light in the red or NIR region of the spectrum (> 600 nm), so that complexes can be irradiated with low energy (i.e., better tissue penetration[6] to treat deep-seated or large tumours and less harmful light than UV). In order to prepare

PSs that absorb in the red or NIR, we decided to use a strategy based on the cyclometalation of ruthenium(II) polypyridyl complexes. Cyclometalation lowers the energy of the triplet metal-to-ligand charge transfer state (^{3}MLCT) and shortens the excited state lifetime of these complexes.[7] Furthermore, the anionic character of the ligand causes a bathochromic shift of the MLCT absorption band of Ru(II) cyclometalated complex.[8] Worthy of note, Chao and co-workers reported drastic improvements in cytotoxicity for Ru(II) complexes bearing C^N ligands with regards to those bearing N^N.[9,10] However, there are few examples of cyclometalated complexes as PDT PSs. Ruiz and co-workers have recently reported some green-absorber Ru(II) complexes active in hypoxic conditions with high phototoxicity indexes (PI > 580).[11] Huang and co-workers prepared a coumarin-modified cyclometalated Ru(II -complex photoactive on both hypoxic and normoxic conditions.[12] Dunbar and co-workers reported a cyclometalated Ru(II) compound with photoactivity at λ = 633 nm (PI = 7).[13] In all the cases, the absorption is red-shifted with regards to the bipyridyl counterpart.

One of the strategies to improve selectivity in tumoral tissues is bioconjugation.[14,15] Nucleotides, peptides, lipids, carbohydrates, and vitamins have been widely used in combination with ruthenium polypyridyl complexes to reach better internalization and selectivity.[16] Nonetheless, scarce examples of antibody-drug conjugates (ADC) with ruthenium have been reported. Our group previously reported a Ru-nanobody conjugate for targeted PDT.[17] Cetuximab (CTX) is a human-mouse chimeric monoclonal antibody (mAb) that targets the epidermal growth factor receptor (EGFR), overexpressed in some tumours. CTX was approved to treat RAS wild-type metastatic colorectal cancer (mCRC) and head and neck squamous cell carcinoma (HNSCC). Maleimide and benzoyl acrylic acid were selected as the functional groups for the CTX-bioconjugation. Maleimide is the representative moiety commonly used for cysteine conjugation. However, the maleimide strategy has some limitations. On the one hand, an acidic pH is recommendable to avoid side reactions. On the other hand, once attached to the cysteine, the conjugate can undergo a rapid retro-Michael addition with another thiol-containing biomolecule (e.g., glutathione), leading to the release of the antibody and the formation of a thioether maleimide.[18,19] Bernardes and co-workers recently reported the use of carbonyl acrylates as efficient and irreversible scaffolds for cysteine conjugation.[20] Therefore, we decided to select both types of functionalization for comparison.

In this work, we report on the synthesis and characterisation of a novel phenylpyridine-based cyclometalated Ru(II) complex with a terminal amino group, and its corresponding maleimide and benzoylacrylic derivatives, as well as their CTX conjugates. All the complexes have been tested as NIR-PSs for PDT with CT-26 cell line and human SQ20B HNSCC cell line.

Results and discussion

Synthesis and characterization.

The ligands **L2-L5** were prepared as displayed in Scheme 1. The synthesis is described in the experimental part and the characterization data are displayed in the SI for both the ligands (Fig. S1-S11) and the complexes (Fig. S12-S29). Direct reaction of the aminopyridine moiety with a carboxylic acid was unsuccessful, as aromatic amines are known to be weak nucleophiles.[21] Therefore, a linker was introduced to separate spatially the cyclometalating ligand and the targeting functional group (i.e., maleimido or benzoyl acrylate). We substituted the amine group of **L1** for a bromine through the Sandmeyer reaction (**L2**),[22] followed by the reaction of the aryl bromide with ethylene diamine under reflux (**L3**).[23] This alkyl amine is much more reactive and easier to functionalize. Finally, we coupled the benzoyl acrylic acid and the maleimide NHS ester to the amino-terminal group to yield the corresponding amides (**L4** and **L5**).

The complexes (**Ru-NH2**, **Ru-Br**, **Ru-BAA,** and **Ru-Mal**) were prepared through the reaction of the corresponding 2-phenylpyridine ligand and $[Ru(bphen)_2Cl_2]$, along with a silver salt ($AgPF_6$) and a base (NMe_4OH) in a CH_2Cl_2/MeOH (5:1 v/v) mixture at 60 °C for 24 h, as shown in Scheme 2.[24] All the Ru(II) complexes were isolated as the PF_6^- salts, purified by column chromatography and characterized by ^1H, ^{19}F, and ^{13}C NMR, and ESI-MS. The purity was assessed by HPLC and by elemental analysis.

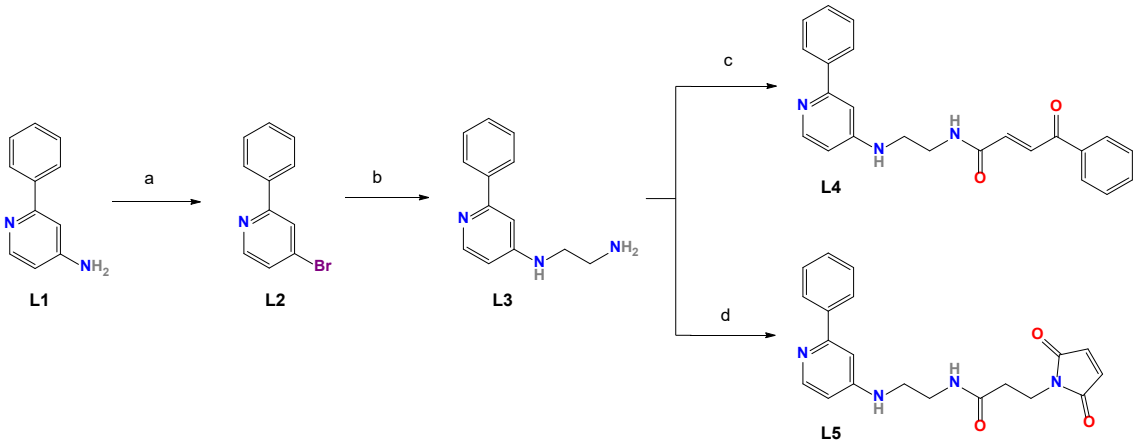

Scheme 1. Synthesis of cyclometalating ligands (**L1-L5**). a) HBr, $NaNO_2$, CuBr, H_2O, rt, overnight; b) ethylenediamine, reflux, 24 h; c) benzoylacrylic acid, HATU, DIPEA, DMF, rt, overnight; d) 3-(Maleimido)propionic acid N-hydroxysuccinimide ester, TEA, DCM, rt, 4 h.

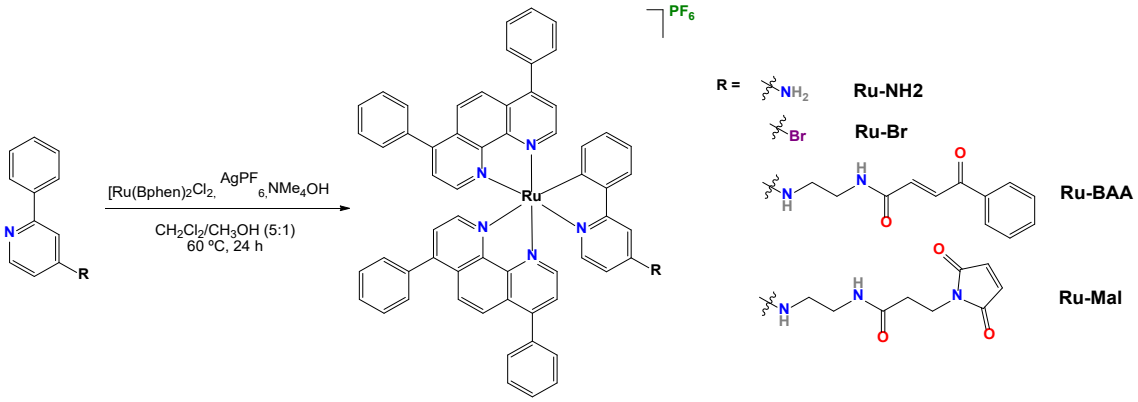

Scheme 2. Schematic synthesis of complexes **Ru-NH_2**, **Ru-Br**, **Ru-BAA** and **Ru-Mal**.

Photophysical properties.

The absorption UV-vis spectra of the complexes were recorded in acetonitrile and are shown in Fig. 1. The complexes show similar patterns and present bands between 250 and 350 nm with absolute maxima at 277-278 nm, corresponding to the spin-allowed π-π* transitions. The shoulder around 320 nm is assigned to ^{1}MLCT and ^{1}LLCT. The broad band appearing over 450 nm is ascribed to the ^{3}MLCT transitions, bathochromic shifted due to cyclometalation. Relative maxima were found around 500 and 580 nm, except for **Ru-Br**, whose maxima are blue-shifted when compared with the amino-derivatives. This observation implies that bromine, as an example of EWG, in *para* to the coordinating N atom blue-shifts the absorption, whereas the amine, as EDG, has the opposite effect. It is important to highlight that all the complexes exhibit absorption at 700 nm, with molar absorptivities shown in Table 1. Furthermore, **Ru-Mal** and **Ru-BAA** functionalized complexes display absorption up to 725 nm with $\varepsilon > 1000$ $M^{-1}cm^{-1}$. The emission spectra

of the complexes were recorded in degassed acetonitrile. As expected, and already reported, cyclometalation causes a rapid decay of the excited states.[9] Thus, the cyclometalated complexes exhibited weak emission (see Fig. 2), with bands centred in the NIR region (764-799 nm). **Ru-Br** was the most emissive complex, 5 times more intense than **Ru-NH2**, and 14 times more than **Ru-BAA** and **Ru-Mal** (Fig. S30). All the absorption and emission data are gathered in Table 1.

Table 1. Photophysical properties of complexes.

Complex	**λ_{max}, nm [ε, $M^{-1}\cdot cm^{-1}$]**	**ε_{700}, $M^{-1}\cdot cm^{-1}$**	**λ_{em}, nm**
Ru-Br	278 [105555], 495 [22974], 544 [22196]	873	764
Ru-NH2	278 [66937], 506 [11361], 582 [15330]	1274	799
Ru-Mal	278 [115339], 506 [20071], 584 [26049]	2302	797
Ru-BAA	277 [107389], 507 [17240], 584 [22436]	2028	796

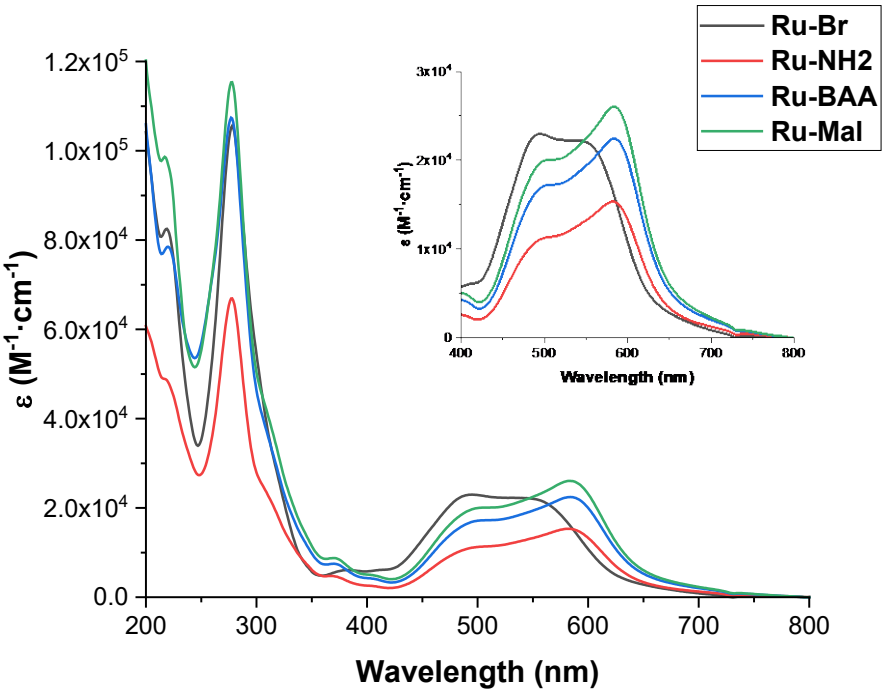

Fig. 1. Absorption spectra of complexes in acetonitrile (10^{-5} M).

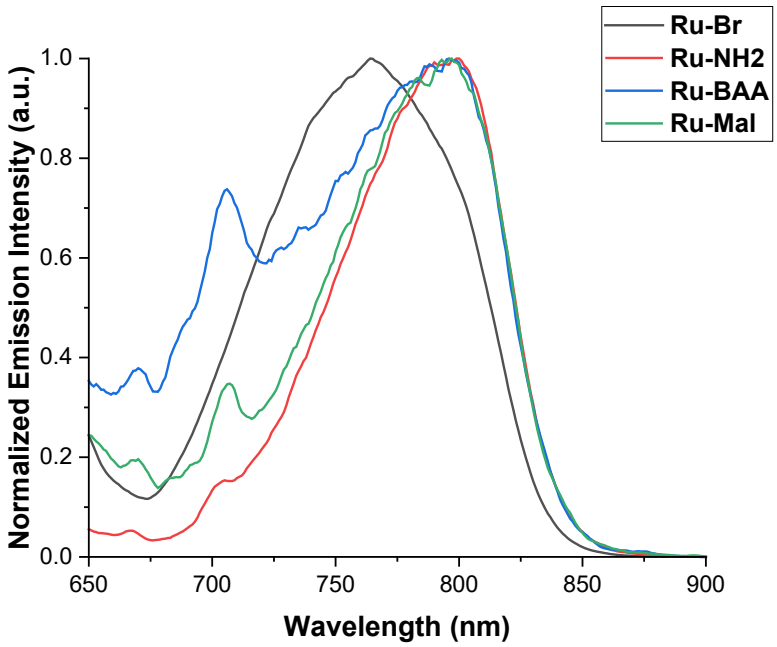

Fig. 2. Emission spectra of complexes in degassed acetonitrile (10^{-5} M).

$^1O_2$ is the main toxic species for a PS working through the type II mechanism. The emission spectrum of **Ru-NH$_2$** was recorded again after leaving the cuvette open to air for 2 h. The emission intensity decreased 1.5 times as a consequence of oxygen quenching (Fig. S31). Therefore, the production of $^1O_2$ upon irradiation of the PSs was quantitatively evaluated in acetonitrile using the direct method of detecting the phosphorescence of $^1O_2$. The quantification of the characteristic luminescence produced by the relaxation of $^1O_2$ (λ_{em}= 1275 nm) was monitored as a function of the irradiation time (λ_{exc} = 450 nm). The $^1O_2$ quantum yield was calculated using $[Ru(bpy)_3]Cl_2$ as a control in acetonitrile. The **Ru-NH$_2$** $^1O_2$ quantum yield (Fig. S32) was 19 % and 77 % for the control. The low yield obtained with the novel ruthenium complex could be explained by the presence of the amine group, which is able to quench the $^1O_2$ generation, as previously reported[25]. One of the explanations for the quenching mechanism is due to a charge transfer between the ground state of a nitrogen-containing compound and $^1O_2$. All in all, we cannot discard the possibility of the PS to undergo type I mechanism.

Phototoxicity Studies of Ru-NH$_2$ on 2D Monolayer Cells

The first step toward the biological investigation of the **Ru-NH$_2$** complex was the evaluation of its photocytotoxicity in monolayer cultures of CT-26 (mouse colon adenocarcinoma) cell line using a fluorometric resazurin cell viability assay.

Protoporphyrin IX (PpIX), clinically approved for PDT, was tested in the same cell line as a positive control. To study its efficiency as a PDT PS, the cytotoxicity of both the complex and the control was tested in the dark and upon irradiation at 670 nm (60 min, 3.75 mW cm^{-2}, 13.5 J cm^{-2}) based on the absorption spectra (Fig. 3 and Fig. S33). Importantly, the Ru(II) complex was found to be nontoxic in the dark (IC_{50}, dark > 100 μM). This is an important requirement for a PDT agent. As desired, it was found to be phototoxic in the lower-micromolar range (IC_{50}, 670 nm = 0.27 ± 0.02 μM). Furthermore, the non-dark cytotoxicity of the ruthenium complex led to excellent phototoxicity indexes (PI) of > 370. PI is defined as the ratio between dark toxicity and phototoxicity. Based on this promising result, we investigated its photocytotoxicity upon irradiation at 740 nm (60 min, 3.50 mW cm^{-2}, 12.6 J cm^{-2}) and 770 nm (60 min, 6.75 mW cm^{-2}, 24.3 J cm^{-2}). Interestingly, **Ru-NH$_2$** was found to be cytotoxic after irradiation with near-infrared light in the micromolar range (IC_{50}, 740 nm = 0.64 ± 0.03 μM, PI = > 156; IC_{50}, 770 nm = 23.7 ± 4.6 μM, PI = > 4). Importantly, we could demonstrate that complex **Ru-NH$_2$** exhibits a phototoxic effect up to 740 nm (see Table S1). To the best of our knowledge, this is one of the first examples of a Ru(II)-NIR PS, highly phototoxic, without using upconverting nanoparticles[26,27], two-photon absorption[28,29] or conjugating it with red-absorbing fluorophores such as BODIPYs[30] or porphyrins[31]. Only scarce examples of Ru(II)-NIR PSs have been reported with low-to-moderate PIs at such wavelengths.[2,32,33] In light of these promising results, the phototoxicity of the targeting ability of two novel cetuximab-conjugates was evaluated in more detail.

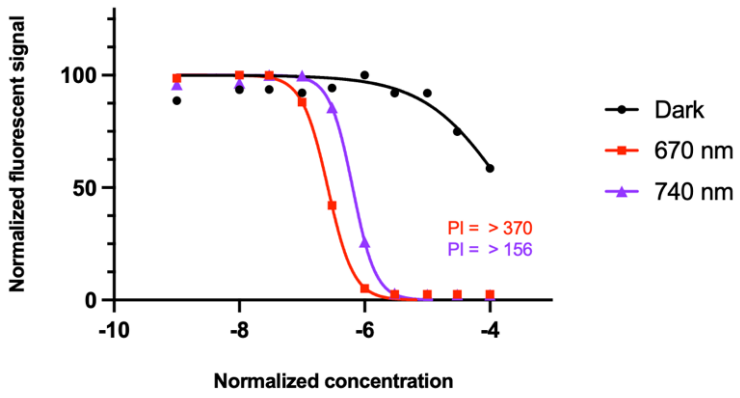

Fig. 3. Dose–response curves of Ru-NH$_2$ in CT-26 cell line in the dark, after excitation at 670 nm and 740 nm.

Ru-CTX bioconjugates

The promising results obtained for the **Ru-NH$_2$** complex prompted us to prepare Antibody-Drug Conjugates (ADCs), using cetuximab (CTX) as the antibody, and applying two different conjugation strategies. We used the well-known and classic maleimido functionalization and a benzoylacrylate as a non-typical, promising conjugation method. Both moieties undergo rapid Michael addition, but the benzoylacrylic derivative is more stable.[20] Nonetheless, CTX has no cysteine moiety available for conjugation. Therefore, in a first step, CTX was combined in PBS (pH = 8.0) with the Traut's reagent (2-iminothiolane, a thiolating agent of primary amines) to thiolate the amino groups from accessible lysins.[34] DTNB (5,5′-dithiobis(2-nitrobenzoic acid) and BCA (bicinchoninic acid) assays were performed to determine the number of thiol groups and the concentration of antibody, respectively (see Table S2, Fig. S34 and S35). The Ru-containing bioconjugates (Scheme 3), **Ru-Mal-CTX,** and **Ru-BAA-CTX**, were prepared by the rection of the thiolated cetuximab (**CTX-SH**) with the corresponding **Ru-Mal** and **Ru-BAA** complexes in different buffer solutions (PBS, pH = 7.4 and NaPi, pH = 7.0, respectively). MALDI-TOF mass spectra were evaluated to determine the number of Ru units per CTX (Table 2 and Fig. 4). These are, to the best of our knowledge, the first CTX-Ru bioconjugates described in literature.

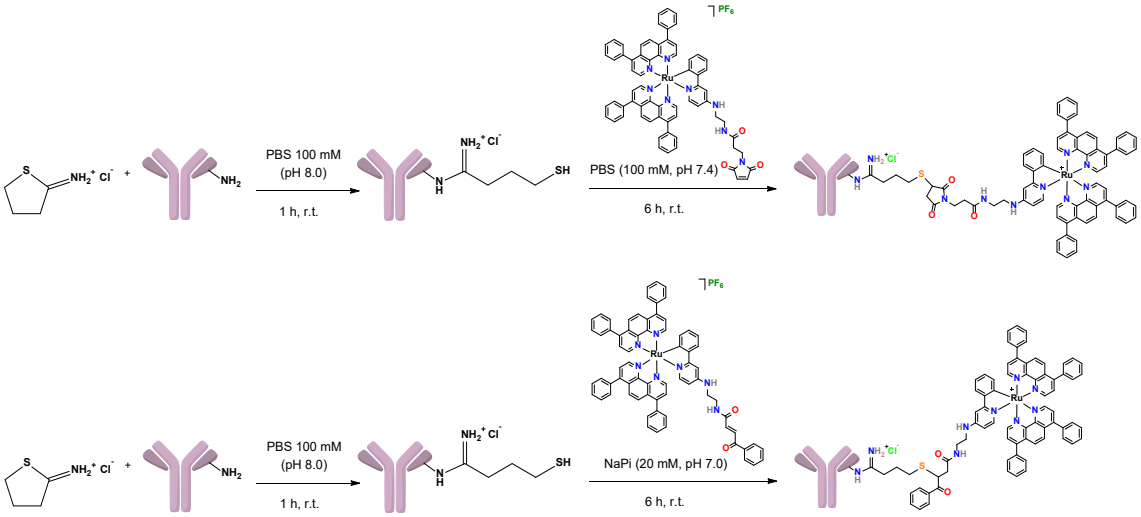

Scheme 3. Representation of the synthesis of the Ru-CTX conjugates. The structure of the conjugates is representative, as there is more than one ruthenium unit per cetuximab.

Table 2. Number of Ru per CTX calculated by MALDI-TOF.

	m/z	CTX-derivative difference	m/z Ru + Traut's fragment	Number of Ru per CTX	Number of SH per CTX
CTX	153423	-	-	-	-

Ru-Mal-CTX	157661	4238	1233.37	4238/1233.37 = 3.44 ~ **3**	CTX-SH-PBS 1.87 ~ **2**
Ru-BAA-CTX	158503	5080	1240.38	5080/1240.38 = 4.10 ~ **4**	CTX-SH-NaPi 1.36 ~ **1**

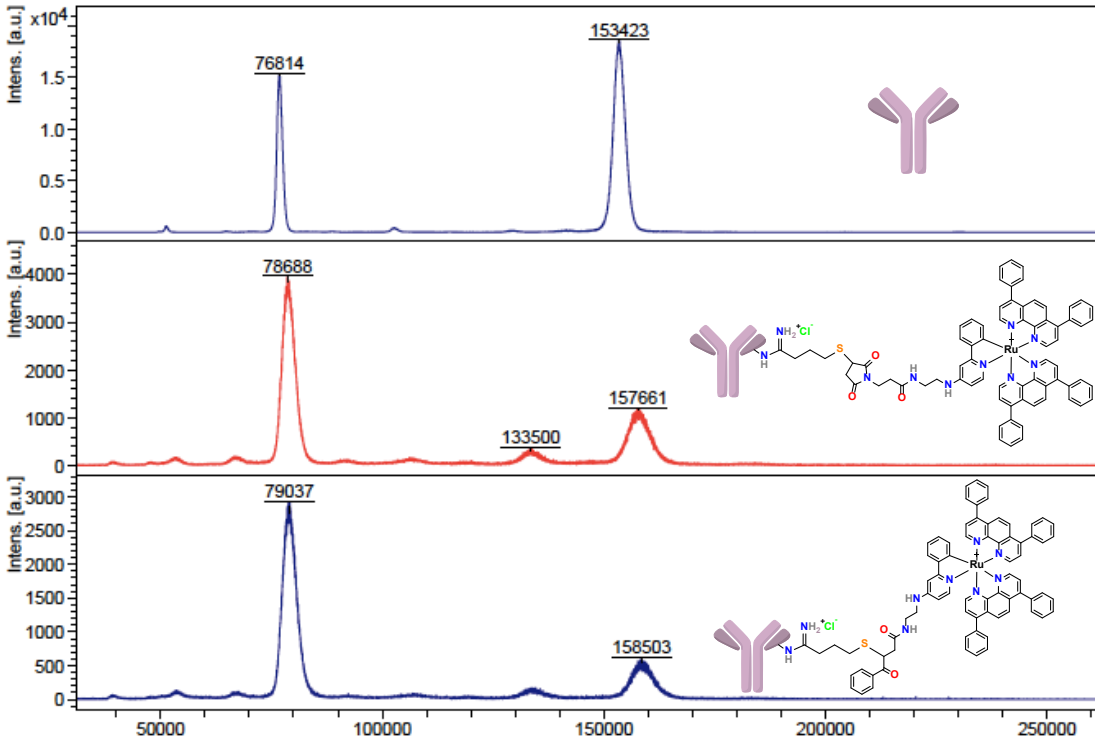

Fig. 4. MALDI-TOF mass spectra of CTX (up), **Ru-Mal-CTX** (middle) and **Ru-BAA-CTX** (down).

Phototoxicity Studies of CTX-Ru bioconjugates on human 2D Monolayer HNSCC Cells

CTX is the only FDA-approved targeted therapy used for the management of recurrent/metastatic locally advanced head and neck squamous cell carcinoma (HNSCC).[35,36] In order to evaluate the efficiency of red-light-based PDT using the **Ru-NH$_2$** complex as well as the **Ru-Mal-CTX** and **Ru-BAA-CTX** bioconjugates as PSs, we chose the human SQ20B HNSCC cell line as a model. Interestingly, SQ20B cells have been described to be resistant to conventional therapy, like radiotherapy,[37] and to EGFR blockade with CTX.[38] We first wanted to measure the phototoxicity of the **Ru-NH$_2$** complex to SQ20B independently of its functionalization to CTX. To this end, SQ20B cells were grown with increasing concentrations of the **Ru-NH$_2$** complex, both in the dark and upon red light irradiation, and cell viability was assessed 48 h after treatment using a MTT assay. The **Ru-NH$_2$** complex was not found to be toxic in the dark (IC_{50} dark > 50

μM; Fig. 5A). However, it was phototoxic in the lower-micromolar range upon illumination (IC_{50} = 0.99 ± 0.31 μM; PI > 50; Fig. 5A and Table S1). These results show that NIR-PDT using the **Ru-NH$_2$** complex as a PS displays interesting phototoxicity toward human HNSCC cells. Ru(II)-based PSs were previously shown to be effective on three different human HNSCC cell lines.[39] However, the complexes were irradiated by visible light (525 nm - green light). To the best of our knowledge, our work is the first study that shows the efficacy of a Ru(II)-based PS in the human HNSCC model.

To further assess the gain in specificity brought by the **Ru-Mal-CTX** and **Ru-BAA-CTX** bioconjugates, we downregulated the expression of EGFR in SQ20B by transfecting cells with a specific siRNA (siEGFR). A western blot analysis of the expression of EGFR in whole protein extracts from transfected cells showed that the siEGFR efficiently reduced the expression of EGFR in SQ20B cells as compared to cells transfected with non-specific siRNA used as a negative control (siCTRL; Fig. S36A). In order to have a more resolutive idea of siRNA-mediated EGFR downregulation at the individual cell level, the expression of EGFR was also assessed with an immunohistochemistry approach: consistently with the results from the western blot analysis, we observed that the expression of EGFR was downregulated in about 90 % of the cells (Fig. S36B). We then analysed the phototoxicity of the **Ru-Mal-CTX** and **Ru-BAA-CTX** bioconjugates on siRNA-transfected SQ20B cells using a cell viability MTT assay. Disappointingly, red-light-based PDT using both bioconjugates only induced a mild reduction of cell viability of SQ20B cells, which was not found to be statistically significant (Fig. 5B). Downregulation of EGFR expression poorly impaired the efficacy of the treatment, and the observed trend was not found to be statistically significant. One possibility to explain this disappointing result could be due to the fact the EGFR expression is still observed in 10 % of the siRNA-transfected cells. Yet, the percentage alone is unlikely to be the only reason to explain the absence of specificity in the treatment. Another explanation could be related to the receptor. The EGFR is found on the cell membrane and therefore the CTX will anchor the receptor without internalizing the cell. Thus, the Ru(II) unit attached to CTX is not able to cross the cell membrane unless it is able to break off from CTX. Therefore, to overcome this problem, we may design the conjugates with longer linker chains, or labile bonds.

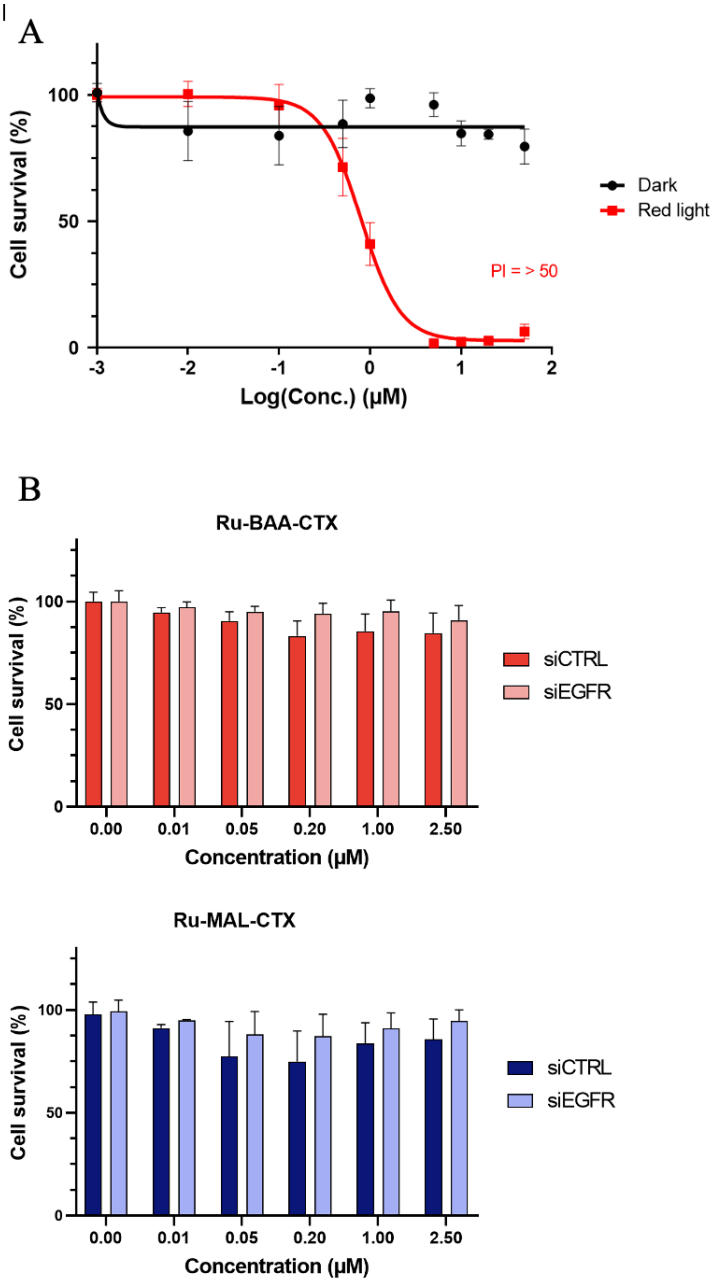

Fig. 5. A. MTT-based analysis of the survival of SQ20B cells treated with **Ru-NH$_2$** in the dark and with red light. B. Analysis of the cell survival of SQ20B transfected with control (siCTRL) or EGFR siRNA (siEGFR) and treated with **Ru-BAA-CTX** or **Ru-MAL-CTX**-based PDT.

Conclusions

In summary, we have reported a Ru(II) PS for PDT, **Ru-NH$_2$**, with excellent phototoxic performance in the near infrared region. To the best of our knowledge, this is one of the first examples of Ru(II) polypyridyl complex that operate in the near infrared range. One of the key factors in the successful design of this PS has been cyclometalation. The

introduction of a cyclometalated ligand in the complex bathochromic shifts the absorption, reaching the infrared region of the spectrum, a fundamental requirement for a good PS for treatment of deep-seated or large tumours. Despite the low generation of $^1O_2$, **Ru-NH$_2$** is able to cause cell death after light irradiation at 740 nm, whereas is nontoxic in the dark (PI > 156). We have also reported two novel Ru(II)-containing bioconjugates with cetuximab, a monoclonal antibody that targets the EGFR, overexpressed in some tumours. The bioconjugation was selected to gain selectively and efficiently target the tumoral tissue. Two different strategies were used to prepare the ADC, the classic maleimide and the recent and innovative benzoylacrylate. However, only a mild effect in the PDT activity of the conjugates was observed without a significant difference between them. In spite of these results, this is the first example of a Ru-CTX conjugate. As future prospects, an improvement in the bioconjugates design is required and could be achieved by extending the length of the linker. Finally, it is important to highlight the relevance of the outstanding phototoxicity of the nude complex. This high PI exclusively comes from the PS without using techniques or strategies other than cyclometalation.

Experimental section

Materials

All the chemicals were purchased from commercial suppliers and were used without further purification. Solvents were dried on a solvent distillation system (SDS). Deuterated solvents Chloroform-d and Methylene Chloride-d were purchased from Eurisotop.

Instrumentation

^{1}H and ^{13}C NMR were recorded on a Bruker 400 MHz NMR spectrophotometer. chemical shifts were internally referenced to TMS via the residual ^{1}H signal of solvents. Chemical shift values are reported in ppm and coupling constants (J) in Hertz. Microanalysis (CHNS) were performed in an Elementar Vario instrument, with two or three repeats per sample. Electrospray ionization-mass spectrometry (ESI-HRMS) experiments were carried out using a LTQ-OrbitrapXL from ThermoScientific (Thermo Fisher Scientific) instrument and operated in positive ionization mode, with a spray voltage at 3.6 kV. A UltrafleXtreme mass spectrometer (Bruker Daltonics, Bremen) was used for all MALDI-TOF experiments. Mass spectra were obtained in linear positive ion mode. The laser

intensity was set just above the ion generation threshold to obtain peaks with the highest possible signal-to-noise (S/N) ratio without significant peak broadening. All data were processed using the FlexAnalysis software package (Bruker Daltonics). Sinapic acid (SA) was used as the matrix. UV−vis absorbance spectra were recorded in a quartz cuvette using a Cary 4000 UV−vis spectrometer (Agilent). Emission spectra were recorded in a FLS980 Edinburgh Instrument. $^1O_2$ luminescence was measured with an infrared detector InGaAs (800 - 1550 nm) via the dual network emission monochromator SPEX (600 lines / mm blazed at 1 μm) and a long-wave pass (780 nm). The singlet oxygen quantum yield was determined by the equation (1):

$$\Phi_{\Delta} = \Phi_{\Delta 0} \cdot \frac{I}{I_0} \cdot \frac{DO_0}{DO} \quad (1)$$

where Φ_Δ and $\Phi_{\Delta o}$, I and I_o, DO and DO_o are the singlet oxygen quantum yield, the singlet oxygen luminescence intensities and the optical densities respectively of the sample and of the standard. The standard used for the singlet oxygen quantum yield was $Ru(bpy)_3$ in acetonitrile with a $\Phi_{\Delta o}$ of 0,77[40]. HPLC analysis was performed using two Agilent G1361 1260 Prep Pump, an Agilent G7115A 1260 DAD WR detector equipped with an Agilent Pursuit XRs 5C18 (100 Å, C_{18} 5 μm 250 × 4.6 mm) column. The flow rate was 1 mL/min with the following gradient: 0−3 min: isocratic 95% A (5% B); 3−17 min: linear gradient from 95% A (5% B) to 0% A (100% B); 17−23 min: isocratic 0% A (100% B). Chromatograms were detected at 215 nm. The solvents (HPLC grade) were Millipore water (0.1 % TFA, solvent A) and acetonitrile (0.1 % TFA, solvent B). The sample was dissolved in 1:1 (v/v) ACN/H_2O 0.1% TFA solution and filtered through a 0.2 mm membrane filter.

Synthesis and characterization

4-bromo-2-phenylpyridine (**L2**). Hydrobromic acid (60 mL, 48 % aqueous solution) and copper bromide (4.22 g, 29.4 mmol) were added over 4-amino-2-phenylpyridine (**L1**, 1 g, 5.88 mmol). The colour immediately changed to purple. An aqueous solution of sodium nitrite (8.11 g in 35 mL) was slowly added, leaving a scape for gases to release. The mixture colour changed to dark brown, and the slurry was left stirring overnight at room temperature. A saturated sodium hydroxide solution was added, and the mixture was extracted with diethyl ether (x3). The organic phase was dried over sodium sulphate, filtered and the solvent was evaporated to dryness to obtain an orange oil. Yield: 97 % (1.33 g, 5.68 mmol). ^{1}H NMR (400 MHz, Chloroform-d) δ 8.50 (dd, J = 5.3, 0.6 Hz, 1H,

H^6), 8.00 – 7.94 (m, 2H, $H^{Ph\text{-}o}$), 7.90 (dd, J = 1.8, 0.6 Hz, 1H, H^3), 7.52 – 7.41 (m, 3H, $H^{Ph\text{-}m}$, $H^{Ph\text{-}p}$), 7.39 (dd, J = 5.3, 1.8 Hz, 1H, H^5) ppm. ^{13}C NMR (101 MHz, Chloroform-d) δ 159.0 (s, 1C), 150.5 (s, 1C), 138.2 (s, 1C), 133.6 (s, 1C), 129.7 (s, 1C), 129.0 (s, 2C), 127.1 (s, 2C), 125.4 (s, 1C), 124.0 (s, 1C) ppm.

N^1-(2-phenyl-4-pyridinyl)-1,2-ethanediamine (**L3**). 4-bromo-2-phenylpyridine (1.329 g, 5.68 mmol) were refluxed over ethylenediamine (20 mL, 370 mmol) for 24 h under nitrogen. The reaction mixture was extracted with dichloromethane and the organic phase was washed once with water and twice with brine. It was dried with sodium sulphate, filtered and the solvent evaporated to dryness to obtain a dark brown oil. Yield: 89 % (1.074 g, 5.04 mmol). ^{1}H NMR (400 MHz, Chloroform-d) δ 8.29 (d, J = 5.7 Hz, 1H), 7.91 (dd, J = 7.0, 1.7 Hz, 2H), 7.48 – 7.34 (m, 3H), 6.88 (d, J = 2.3 Hz, 1H), 6.44 (dd, J = 5.7, 2.3 Hz, 1H), 4.74 (s, 1H), 3.27 (q, J = 5.7 Hz, 2H), 3.00 (t, J = 5.9 Hz, 2H) ppm.

(E)-4-oxo-4-phenyl-N-(2-((2-phenyl-4-pyridinyl)amino)ethyl)-2-butenamide (**L4**). Benzoyl acrylic acid (753 mg, 4.26 mmol) was dissolved in anhydrous dimethyl formamide (15 mL, degassed). HATU (1.87 g, 4.92 mmol) and DIPEA (2.0 mL, 11.5 mmol) were added, and the reaction was left stirring at rt for 2 h. N^1-(2-phenyl-4-pyridinyl)-1,2-ethanediamine (413 mg, 1.9 mmol) was dissolved in dimethyl formamide (10 mL), and DIPEA was added (3.9 mL, 22.4 mmol). The amino solution was transferred into the acid one, and the rest of the DIPEA (2.0 mL, 11.5 mmol) was added. The reaction was left stirring overnight at rt. The solvent was evaporated to dryness and dichloromethane was used to dissolve the product, which was then washed with water (x1) and brine (x2). After drying with sodium sulphate and filtrating, the solvent was evaporated to dryness. The product was purified by column chromatography in DCM (dichloromethane)/MeOH/NH_3 (80:10:1) to yield a white solid. Yield: 12 % (85 mg, 0.23 mmol). ^{1}H NMR (400 MHz, Chloroform-d) δ 8.15 (d, J = 5.6 Hz, 1H), 8.00 – 7.88 (m, 3H), 7.86 – 7.75 (m, 2H), 7.57 (td, J = 7.6, 1.2 Hz, 1H), 7.45 (t, J = 7.8 Hz, 2H), 7.40 – 7.30 (m, 4H), 6.99 (d, J = 15.1 Hz, 1H), 6.78 (d, J = 2.3 Hz, 1H), 6.35 (dd, J = 5.8, 2.1 Hz, 1H), 5.34 (s, 1H), 3.57 (q, J = 5.8 Hz, 2H), 3.34 (q, J = 5.1 Hz, 2H) ppm. ^{13}C NMR (101 MHz, Chloroform-d) δ 165.5, 162.7, 157.8, 154.4, 149.3, 139.7, 136.9, 135.3, 133.9, 133.3, 129.0, 128.9, 128.7, 127.1, 106.3, 104.9, 43.0, 39.2, 38.7, 36.6, 31.6 ppm.

3-(2,5-dioxo-2,5-dihydro-1H-pyrrol-1-yl)-N-(2-((2-phenyl-4-pyridinyl)amino)ethyl) propenamide (**L5**). N^1-(2-phenyl-4-pyridinyl)-1,2-ethanediamine (555 mg, 2.6 mmol) was dissolved in dichloromethane (degassed, 20 mL) and TEA (0.4 mL, 2.9 mmol) was added. Separately, 3-(Maleimido)propionic acid N-hydroxysuccinimide ester (630 mg, 2.4 mmol) was dissolved in dichloromethane (degassed, 20 mL) and when completely dissolved, the solution was transferred to the previous one. The reaction was tracked by TLC in DCM/MeOH/NH_3 (80:10:1) until completion after 3.5 h. The solvent was evaporated to dryness and the residue redissolved in dichloromethane and washed with water (x1) and brine (x2). After drying the organic phase with sodium sulphate and filtering, the solvent was evaporated to dryness. Yield: 60 % (528 mg, 1.45 mmol). ^{1}H NMR (400 MHz, Chloroform-d) δ 8.28 (d, J = 5.7 Hz, 1H), 8.00 – 7.87 (m, 2H), 7.48 – 7.34 (m, 4H), 6.86 (d, J = 2.2 Hz, 1H), 6.60 (s, 1H), 6.40 (dd, J = 5.7, 2.3 Hz, 1H), 3.84 (t, J = 6.7 Hz, 2H), 3.54 (q, J = 5.9 Hz, 2H), 3.33 (q, J = 5.3 Hz, 2H), 2.56 (t, J = 6.8 Hz, 2H) ppm. ^{13}C NMR (101 MHz, Chloroform-d) δ 171.3, 170.7, 158.2, 154.2, 150.1, 140.1, 134.3, 128.8, 128.7, 127.1, 106.2, 104.7, 43.6, 38.9, 35.1, 34.5 ppm.

[Ru(bphen)$_2$Cl$_2$]. [Ru(dmso)$_4$Cl$_2$] (2 g, 4.1 mmol), bathophenanthroline (bphen, 2.88 g, 8.7 mmol) and LiCl (1.23 g, 28.9 mmol) were dissolved in anhydrous DMF under inert atmosphere and refluxed at 150 °C for 24 h. The mixture was cooled to rt and some DMF was evaporated. Cold acetone was added, and the mixture was left in the fridge overnight to favour precipitation. The crystalline solid was filtered and washed with lots of water, acetone and diethyl ether to yield a purple solid. Yield: 65 % (2.27 g, 2.7 mmol).

[Ru(bphen)$_2$(L1)]PF$_6$. **Ru-NH$_2$**. [Ru(bphen)$_2$Cl$_2$] (120 mg, 0.14 mmol) was dissolved in a DCM/MeOH (5:1) mixture under inert atmosphere and protected from light. $AgPF_6$ (83 mg, 0.33 mmol) was added and after 2 h stirring at rt, 4-amino-2-phenylpyridine (26 mg, 0.15 mmol) and NMe_4OH (16 mg, 0.18 mmol). The mixture was refluxed overnight. The dark pink solution was cannula-filtered to remove silver salts and the solvent was evaporated to dryness. The crude product was purified by column chromatography on silica in DCM/ACN (50:1) and dried under vacuum to obtain a purple solid. Yield: 53 % (80 mg, 0.074 mmol). ^{1}H NMR (400 MHz, Methylene Chloride-d2) δ 8.68 (d, J = 5.6 Hz, 1H), 8.50 (d, J = 5.6 Hz, 1H), 8.21 (d, J = 5.3 Hz, 1H), 8.14 (s, 2H), 8.15 – 8.04 (m, 3H), 7.76 (d, J = 6.8 Hz, 1H), 7.65 – 7.52 (m, 23H), 7.39 (d, J = 5.5 Hz, 1H), 7.28 (d, J = 2.4 Hz, 1H), 7.16 (d, J = 6.4 Hz, 1H), 6.92 (td, J = 7.7, 1.2 Hz, 1H), 6.81 (td, J = 7.3, 1.2 Hz,

1H), 6.51 (d, J = 6.6 Hz, 1H), 6.26 (dd, J = 6.4, 2.6 Hz, 1H), 4.58 (s, 2H) ppm. ^{13}C NMR (101 MHz, Methylene Chloride-d2) δ 167.4, 154.7, 154.0, 150.7, 150.4, 150.3, 149.2, 147.8, 147.7, 146.5, 146.3, 145.0, 137.1, 137.0, 136.2, 130.4, 130.3, 130.2, 129.9, 129.8, 129.59, 129.57, 129.2, 128.91, 128.89, 128.83, 128.80, 126.4, 126.2, 126.1, 126.0, 125.8, 124.0, 121.6, 109.7, 104.8 ppm. ^{19}F NMR (376 MHz, Methylene Chloride-d2) δ -73.33 (d, J_{F-P} = 710.7 Hz, 6F) ppm.

Anal. Calcd for $C_{59}H_{41}N_6PF_6Ru\cdot(H_2O)_{0.75}$: C 64.80; H 3.92; N 7.68; Found: C 64.86; H 3.90; N 7.71.

HRMS (ESI) m/z: [M]+ Calcd for $C_{59}H_{41}N_6Ru$ 935.2431. Found 935.2433; (Error: 0.2 ppm).

[Ru(bphen)$_2$(L2)]PF$_6$. **Ru-Br**. [Ru(bphen)$_2$Cl$_2$] (418 mg, 0.50 mmol) was dissolved in 10 mL of a DCM/MeOH (5:1) mixture under inert atmosphere and protected from light. $AgPF_6$ (290 mg, 1.15 mmol) was added and after 30 min stirring at rt, 4-bromo-2-phenylpyridine (129 mg, 0.55 mmol) and NMe_4OH (55 mg, 0.60 mmol). The mixture was refluxed overnight. The dark red solution was cannula-filtered to remove silver salts and the solvent was evaporated to dryness. The crude product was purified by column chromatography on silica in DCM/ACN (20:1) to obtain a pink-purple solid, which was washed with diethyl ether and dried under vacuum. Yield: 28 % (158 mg, 0.14 mmol). ^{1}H NMR (400 MHz, Methylene Chloride-d2) δ 8.54 (d, J = 5.6 Hz, 1H), 8.37 (d, J = 5.5 Hz, 1H), 8.23 (d, J = 5.3 Hz, 1H), 8.18 (d, J = 2.1 Hz, 1H), 8.16 (s, 2H), 8.12 (d, J = 2.0 Hz, 2H), 8.03 (d, J = 5.5 Hz, 1H), 7.87 (d, J = 7.5 Hz, 1H), 7.64 (d, J = 5.3 Hz, 1H), 7.63 – 7.51 (m, 23H), 7.44 (d, J = 5.5 Hz, 1H), 7.05 (dd, J = 6.1, 2.1 Hz, 1H), 6.98 (t, J = 7.4 Hz, 1H), 6.88 (t, J = 6.8 Hz, 1H), 6.59 (d, J = 7.4 Hz, 1H). ^{13}C NMR (101 MHz, Methylene Chloride-d2) δ 169.6, 155.3, 151.5, 150.6, 150.2, 150.1, 149.3, 149.0, 148.5, 147.4, 147.2, 146.0, 145.9, 136.87, 136.85, 136.7, 136.5, 132.5, 130.34, 130.30, 130.2, 130.0, 130.0, 129.8, 129.7, 129.6, 129.3, 129.1, 129.0, 128.9, 126.7, 126.5, 126.3, 126.23, 126.16, 126.1, 126.0, 125.8, 125.3, 122.9, 121.9 ppm. ^{19}F NMR (376 MHz, Methylene Chloride-d2) δ -73.52 (d, J_{F-P} = 710.7 Hz, 6F) ppm.

HRMS (ESI) m/z: [M]+ Calcd for $C_{59}H_{39}BrN_5Ru$ 998.1427. Found 998.1441; (Error: 1.4 ppm).

[Ru(bphen)$_2$(L4)]PF$_6$. **Ru-BAA**. [Ru(bphen)$_2$Cl$_2$] (90 mg, 0.11 mmol) and $AgPF_6$ (63 mg, 0.25 mmol) were suspended in a DCM/MeOH (5:1, 6 mL) mixture under nitrogen

and protected from light. After stirring for 1 h, a solution of the ligand **L4** (44 mg, 0.12 mmol) in DCM/MeOH (5:1, 4 mL) and the base NMe_4OH (12 mg, 0.13 mmol) were added. The mixture was refluxed overnight. After completion of the reaction, the solution was filtered, and the solvent evaporated to dryness. The purple crude was purified by column chromatography on alumina in DCM/acetone (gradient from 1 % to 10 % acetone). Yield: 9 % (13 mg, 0.01 mmol). ^{1}H NMR (400 MHz, Methylene Chloride-d2) δ 8.52 (bs, 1H), 8.31 – 8.03 (m, 7H), 7.98 – 7.91 (m, 3H), 7.82 (d, J = 15.2 Hz, 2H), 7.71 – 7.50 (m, 28H), 7.46 (dd, J = 8.3, 7.1 Hz, 2H), 7.37 – 7.24 (m, 1H), 7.21 – 7.03 (m, 1H), 6.88 (d, J = 15.2 Hz, 1H), 6.60 (t, J = 6.1 Hz, 1H), 5.92 (bs, 1H), 3.63 (q, J = 6.0 Hz, 2H), 3.51 (m, 2H). ^{19}F NMR (376 MHz, Methylene Chloride-d2) δ -73.10 (d, J = 711.3 Hz).
Anal. Calcd for $C_{71}H_{52}N_7O_2PF_6Ru\cdot(H_2O)$: C 65.63; H 4.19; N 7.55; Found: C 65.38; H 4.06; N 7.40.
HRMS (ESI) m/z: [M]+ Calcd for $C_{71}H_{52}N_7O_2Ru$ 1136.3220. Found 1136.3242; (Error: 1.9 ppm).

$[Ru(bphen)_2(L5)]PF_6$. **Ru-Mal**. This complex was synthesised in the same manner as **Ru-BAA**, using $[Ru(bphen)_2Cl_2]$ (130 mg, 0.16 mmol), $AgPF_6$ (91 mg, 0.36 mmol), **L5** (62 mg, 0.19 mmol) and NMe_4OH (17 mg, 0.19 mmol). The purple crude was purified by column chromatography on alumina in DCM/ACN (gradient from 50:1 to 5:1). Yield: 10 % (20 mg, 0.024 mmol). ^{1}H NMR (500 MHz, Methylene Chloride-d2) δ 8.27 – 8.15 (m, 4H), 8.05 (d, J = 9.5 Hz, 1H), 8.00 (s, 1H), 7.92 (s, 1H), 7.76 (s, 1H), 7.69 (t, J = 7.6 Hz, 2H), 7.65 – 7.59 (m, 9H), 7.59 – 7.52 (m, 8H), 7.52 – 7.44 (m, 4H), 7.02 (s, 1H), 6.75 (s, 1H), 6.60 (s, 2H), 6.18 (t, J = 6.1 Hz, 1H), 5.05 (s, 1H), 3.75 (t, J = 6.9 Hz, 2H), 3.53 (s, 2H), 3.44 (t, J = 5.8 Hz, 2H), 2.46 (t, J = 7.0 Hz, 2H).
Anal. Calcd for $C_{68}H_{51}N_8O_3PF_6Ru\cdot(H_2O)_3$: C 61.49; H 4.33; N 8.44; Found: C 61.62; H 3.96; N 8.28.
HRMS (ESI) m/z: [M]+ Calcd for $C_{68}H_{51}N_8O_3Ru$ 1129.3122. Found 1129.3144; (Error: 1.9 ppm).

CTX-SH. In an Eppendorf tube, 200 µL of cetuximab (CTX, 5 mg/mL), 33 µL of Traut's reagent (2-iminothiolane, 1 mM) and 750 µL of PBS (pH 8.0, 0.1 M, 0.5 mM EDTA) were stirred for 1 h at rt. Excess of Traut's reagent was removed by overnight dialysis in PBS (pH 7.4, 0.1 M) or NaPi (pH 7.0, 20 mM). The number of thiol groups in CTX-SH were determined by the DTNB assay. 250 µL of CTX-SH, 1 mL of PBS (pH 7.4, 0.1 M)

or NaPi (pH 7.0, 20 mM) and 50 µL of 4 mg/mL Ellman's reagent were incubated for 15 min, and the absorbance was recorded at 412 nm. L-cysteine (0-12.5 µM) was used as a standard for calibration. The concentration of CTX and CTX-SH was determined by the BCA assay. 0.1 mL of standard (BSA) or sample solution and 2 mL of working reagent (50 parts of reagent A and 1 part of reagent B) were incubated at 37 °C for 30 min. After cooling and within 10 min, the absorbance was recorded at 562 nm. Standard BSA solutions (0-2000 µg/mL) were used for calibration.

CTX-Ru-Mal and CTX-Ru-BAA. The ruthenium-CTX conjugates were prepared by reacting the thiolated Ab, CTX-SH (50 µL) with the corresponding **Ru-Mal** or **Ru-BAA** (1 µL, 5 mM in DMF), TCEP (5 µL, 10 mM), DMF (24 µL) in 200 µL of buffer (PBS = pH 7.4, 0.1 M or NaPi = pH 7.0, 20 mM, respectively). After incubation with stirring at rt ~~r.t.~~ for 6 h, the excess of Ruthenium complex was removed by overnight dialysis in the corresponding buffers (PBS for the maleimido conjugate and NaPi for the benzoyl acrylic acid derivative). MALDI-TOF was run to determine the mass and the number of Ruthenium units per CTX.

DTNB Assay – concentration of thiols

A calibration curve was prepared taking L-cysteine as a reference of thiols. Six solutions were prepared using 0-12.5 µL of L-cysteine (2 mM), 50 µL of Ellman's reagent (4 mg/mL) and completing volume with PBS buffer to get 1000 µL. After 15 min, the colourless samples changed to yellowish and the absorption spectra of both the calibration and the samples were recorded. Absorption at 412 nm vs concentration of L-cysteine was plotted to obtain the calibration curve adjusted to a linear fit.

BCA Assay – concentration of CTX

A calibration curve was prepared using BSA as the protein. The protocol was followed as stated by Thermo Fisher Scientific®. Nine standard solutions of BSA were prepared (0-2 mg/mL) using solution A - solution B in 50:1. After mixing both solutions and incubate for 30 min at 37 °C, the absorption spectra of the samples were recorded in the next 10 min. Absorption at 562 nm vs concentration of BSA was plotted to obtain the calibration curve.

Estimation of the number of thiol groups

The number of thiol groups per unit of bioconjugate were calculated as the coefficient of the concentration of CTX and the concentration of CTX or Ru-CTX conjugate.

$$Number\ of\ SH\ per\ Ab = \frac{[CTX]}{[SH]}$$

Phototoxicity Studies of Ru-NH_2 on 2D Monolayer Cells

Cell Culture

The CT-26 cell line was cultured in DMEM media (Gibco) supplemented with 10% fetal calf serum (Gibco) and 1% Penicillin-Streptomycin antibiotic (Gibco). Cell lines were maintained in a humidified atmosphere at 37 °C with 5% CO_2.

Phototoxicity

Cells were seeded at a 4,000 cells/well density in 96-well plates (100 µL/well) and were incubated at 37 °C, 5% CO_2 for 24 h. The medium was replaced by test compound dilutions in fresh medium (100 µL/well), and cells were incubated at 37 °C, 5% CO_2 for 4 h. The medium was replaced with 100 µL of fresh medium. Plates were then irradiated at the corresponding wavelength for 1 h using a LUMOS-BIO photoreactor (Atlas Photonics). As a control, a plate was kept in the dark for the same amount of time at 37°C, 0% CO_2. Cells were then incubated for an additional 44 h at 37 °C, 5% CO_2. The medium was replaced with 100 µL of fresh medium containing resazurin (0.2 mg/mL). After 4 h of incubation at 37 °C, 5% CO_2, plates were read using a Cytation 5 (Agilent) Cell Imaging Multimode Reader (λ_{exc} = 540 nm; λ_{read} = 590 nm). Fluorescence data were normalized, data were fitted using GraphPad Prism Software, and IC_{50} was calculated by non-linear regression.

Phototoxicity Studies of CTX-Ru bioconjugates on human 2D Monolayer HNSCC Cells

Cell Culture

The laryngeal squamous cell carcinoma cell line SQ20B was cultured in DMEM medium (D. Dutcher) added with 10% of inactivated fetal bovine serum (Gibco). Cells were grown at 37 °C in a humidified atmosphere containing 5% CO_2.

Phototoxicity of Ru-NH_2

4,000 cells/well (100 µL/well) were seeded in 96-well plates and incubated at 37 °C, 5 % CO_2 for 24 h. Cells were then treated with a range of increasing concentrations of **Ru-NH_2** diluted in medium and incubated for 4 h at 37 °C. Medium was then replaced and cells were exposed to red light for 1h using the Photograph Fill Light MFL-06R, Moman® with the following settings: 25% intensity, Current color (H):360° and saturation (S)=100. As a control, an identical culture plate was kept in the dark. 44 h after illumination, the medium was replaced by 100 µL of a 10 % MTT solution (5 mg/mL bromide 3-(4,5-dimethylthiazol-2-yl)-2,5-diphenyl tetrazolium, Sigma Aldrich) diluted in medium. Cells were incubated 1 h at 37 °C before replacing MTT with 100 µL of DMSO (VWR Chemicals). Plates were stirred at room temperature to ensure that all crystals were dissolved, and absorbance was then read at 590 nm (Tristar^2 Multimode Reader LB942, Berthold Technologies®). Dose-response curves were obtained from nonlinear regression using GraphPad Prism Software.

EGFR expression downregulation

Cells were seeded in 6-well plates at a density of 125,000 cells/well (2 mL/well) and were incubated at 37 °C, 5% CO_2 for 48 h. Cells were transfected with a specific small interfering RNA (siRNA) targeting EGFR (Ambion) or a non-specific siRNA used as a negative control (Ambion), at a final concentration of 5, 10 or 20 nM with the transfecting agent Lipofectamine RNAiMAX (Invitrogen). Medium was replaced 6 h after transfection and cells were kept at 37 °C for 18 h.

SDS-PAGE and western blot analysis

Total protein extraction was carried out by homogenizing 1.10^6 cells in 100 µL of 1X lysis buffer [1X NP40, 50mM Tris, 150mM NaCl, 1X protease inhibitor, Sigma]. 15 µg of total proteins were resolved by 6 %-12 % gradient SDS-PAGE according to standard methods. Proteins were detected with primary antibodies raised against EGFR (D38B1, rabbit mAb, 1:2,000, Cell Signaling) and GAPDH (6C5, mouse mAb, 1:2,000, Santa Cruz). Blots were probed with secondary antibodies (1:8,000 anti-mouse IgG-HRP linked antibody, Cell Signaling, 7076; 1:10,000 anti-rabbit IgG-HRP linked antibody, Cell Signaling, 7074) Proteins were visualized with enhanced chemiluminescence using the Clarity™ ECL Western blotting Substrate Bio-Rad reagent, according to the manufacturer instructions. Signals were acquired on a Pxi Imager (Syngene®).

Immunofluorescence staining

Cells were seeded on coverslips at a 100,000 cells/well density in 12-well plates (1 mL/well) for 24 h and transfected as described above, with a siRNA final concentration of 5 nM. Cells were fixed with 4 % PFA for 10 min and permeabilized with 0.1 % Triton 1X PBS for 5 min at rt ~~room temperature~~. Saturation of specific sites was achieved with 5 % Normal Goat Serum for 30 min at room temperature. Cells were incubated with an anti-EGFR antibody (D38B1, rabbit mAb, 1:500, Cell Signaling) 4 h at 4 °C and then washed three times in 1X PBS. Coverslips were further incubated with a goat anti-rabbit-alexa488 secondary antibody (A11034, 1:1,000, Invitrogen). After 3 washes in 1X PBS, nuclei were labeled with a DAPI (4',6-diamidino-2-phenylindole) solution (1:20,000) for 5 min, and coverslips were mounted in Calbiochem FluorSave^{TM} reagent (Merck Millipore). Pictures were taken with a Zeiss Axio Imager M2-Apotome2 fluorescence microscope.

Phototoxicity of CTX-Ru bioconjugates

4,000 transfected cells/well (100 µL/well) were seeded in 96-well plates and incubated at 37 °C, 5 % CO_2 for 24 h. Then, cells were treated with different concentrations of **Ru-BAA-CTX** and **Ru-Mal-CTX** diluted in medium for 15 min. Cells were washed twice quickly and once 5 min with medium before light exposure as previously described. A MTT cell viability assay was carried out as described above.

ASSOCIATED CONTENT

Supporting Information available. Characterization of ligands and complexes (^{1}H, ^{13}C and ^{19}F NMR spectra, mass spectra and HPLC chromatograms), photophysical properties, additional biological experiments, and characterization of the bioconjugates (DOC).

Conflicts of interest

The authors declare that they have no conflict of interest.

Aknowledgements

The European Commission H2020-MSCA-IF-2018 grant supported this work, OrganometRuPDT (839499) to M.M. This work was financially supported by an ERC

Consolidator Grant PhotoMedMet to G.G. (GA 681679) and has received support under the program ‘‘Investissements d’Avenir’’ launched by the French Government and implemented by the ANR with the reference ANR-10-IDEX-0001-02 PSL (G.G.), by the ITMO Cancer AVIESAN (Alliance Nationale pour les Sciences de la Vie et de la Sante/ National Alliance for Life Sciences & Health) within the framework of the Cancer Plan (G.G, C.G and A.J.). A.G thanks the ARC Foundation for cancer research for a postdoctoral research fellowship. The Streinth Team is supported by the Association pour la Recherche sur le Cancer, European action COST Proteocure, the Interdisciplinary thematic Institute InnoVec, the IDEX Excellence grant from Unistra, Itmo Cancer, and the Institut National du Cancer. C.T. is financially supported by a PhD fellowship awarded by the Doctoral School ED414 of the University of Strasbourg.

Keywords: Antibody; Bioconjugation; Cetuximab; Metals in Medicine; Photodynamic Therapy; Ruthenium.

Abbreviations

Ab: antibody; ACN: acetonitrile; ADC: antibody drug conjugates; BCA: bicinchoninic acid; BSA: bovine serum albumin; CRC: colorectal cancer; CTX: cetuximab; DAPI: 4',6-diamidino-2-phenylindole; DCM: dichloromethane; DIPEA: N,N-diisopropiletilamina; DMF: N,N-dimethyl formamide; DMSO: dimethyl sulfoxide; DTNB: 5,5′-dithiobis(2-nitrobenzoic acid) / Ellman's reagent; EDG: electron donating group; EGFR: epidermal growth factor receptor; ESI-MS: electrospray ionization mass spectrometry; EWG: electron withdrawing group; HATU: 1-[Bis(dimethylamino)methylene]-1H-1,2,3-triazolo[4,5-b]pyridinium 3-oxide hexafluorophosphate; HNSCC: head and neck squamous cell carcinoma; HPLC: high performance liquid chromatography; HRMS: high resolution mass spectrometry; mAb: monoclonal antibody; MeOH: methanol; MTT: bromide 3-(4,5-dimethylthiazol-2-yl)-2,5-diphenyl tetrazolium; NaPi: sodium phosphate buffer; NIR: near infrared; PBS: Phosphate buffered solution; PDT: photodynamic therapy; PS: photosensitizer; siRNA: small interfering RNA; TCEP: tris(2-carboxyethyl)phosphine.

References

[1] J. Karges, *Angew Chem Int Ed* **2022**, *61*, e202112236.

[2] S. Monro, K. L. Colón, H. Yin, J. Roque, P. Konda, S. Gujar, R. P. Thummel, L. Lilge, C. G. Cameron, S. A. McFarland, *Chem Rev* **2019**, *119*, 797–828.
[3] S. A. McFarland, A. Mandel, R. Dumoulin-White, G. Gasser, *Curr Opin Chem Biol* **2020**, *56*, 23–27.
[4] T. Inc., "TLD-1433 Clinical Trial," can be found under https://clinicaltrials.gov/ct2/show/NCT03945162, (accessed the 11/03/2023).
[5] L. Conti, E. Macedi, C. Giorgi, B. Valtancoli, V. Fusi, *Coord Chem Rev* **2022**, *469*, 214656.
[6] V. v. Barun, A. P. Ivanov, A. v. Volotovskaya, V. S. Ulashchik, *J Appl Spectrosc* **2007**, *74*, 430–439.
[7] H. Huang, P. Zhang, B. Yu, Y. Chen, J. Wang, L. Ji, H. Chao, *J Med Chem* **2014**, *57*, 8971–8983.
[8] P. G. Bomben, K. C. D. Robson, B. D. Koivisto, C. P. Berlinguette, *Coord Chem Rev* **2012**, *256*, 1438–1450.
[9] H. Huang, P. Zhang, H. Chen, L. Ji, H. Chao, *Chem – Eur J* **2015**, *21*, 715–725.
[10] H. Huang, P. Zhang, B. Yu, Y. Chen, J. Wang, L. Ji, H. Chao, *J Med Chem* **2014**, *57*, 8971–8983.
[11] F. J. Ballester, E. Ortega, D. Bautista, M. D. Santana, J. Ruiz, *Chem Comm* **2020**, *56*, 10301–10304.
[12] Z. Lv, H. Wei, Q. Li, X. Su, S. Liu, K. Y. Zhang, W. Lv, Q. Zhao, X. Li, W. Huang, *Chem Sci* **2018**, *9*, 502–512.
[13] B. Peña, A. David, C. Pavani, M. S. Baptista, J.-P. Pellois, C. Turro, K. R. Dunbar, *Organometallics* **2014**, *33*, 1100–1103.
[14] G. T. Hermanson, *Bioconjugate Techniques*, Elsevier, **2013**, pp. 1–125.
[15] S. B. Gunnoo, A. Madder, *Org Biomol Chem* **2016**, *14*, 8002–8013.
[16] M. Martínez-Alonso, G. Gasser, *Coord Chem Rev* **2021**, *434*, 213736.
[17] J. Karges, M. Jakubaszek, C. Mari, K. Zarschler, B. Goud, H. Stephan, G. Gasser, *ChemBioChem* **2020**, *21*, 531–542.
[18] N. Jain, S. W. Smith, S. Ghone, B. Tomczuk, *Pharm Res* **2015**, *32*, 3526–3540.
[19] K. Renault, J. W. Fredy, P.-Y. Renard, C. Sabot, *Bioconjug Chem* **2018**, *29*, 2497–2513.
[20] B. Bernardim, M. J. Matos, X. Ferhati, I. Compañón, A. Guerreiro, P. Akkapeddi, A. C. B. Burtoloso, G. Jiménez-Osés, F. Corzana, G. J. L. Bernardes, *Nat Protoc* **2019**, *14*, 86–99.
[21] W. A. Henderson, C. J. Schultz, *J Org Chem* **1962**, *27*, 4643–4646.
[22] W. W. Weare, R. R. Schrock, A. S. Hock, P. Müller, *Inorg Chem* **2006**, *45*, 9185–9196.
[23] R. Vinck, A. Gandioso, P. Burckel, B. Saubaméa, K. Cariou, G. Gasser, *Inorg Chem* **2022**, *61*, 13576–13585.
[24] M. Albrecht, M. M. Lindner, *Dalton Trans* **2011**, *40*, 8733.
[25] R. H. Young, R. L. Martin, D. Feriozi, D. Brewer, R. Kayser, *Photochem Photobiol* **1973**, *17*, 233–244.
[26] H. Shi, T. Fang, Y. Tian, H. Huang, Y. Liu, *J Mater Chem B* **2016**, *4*, 4746–4753.
[27] P. Hu, T. Wu, W. Fan, L. Chen, Y. Liu, D. Ni, W. Bu, J. Shi, *Biomaterials* **2017**, *141*, 86–95.
[28] F. Heinemann, J. Karges, G. Gasser, *Acc Chem Res* **2017**, *50*, 2727–2736.
[29] H. Huang, B. Yu, P. Zhang, J. Huang, Y. Chen, G. Gasser, L. Ji, H. Chao, *Angew Chem Int Ed* **2015**, *127*, 14255–14258.

[30] L. Qiao, J. Liu, Y. Han, F. Wei, X. Liao, C. Zhang, L. Xie, L. Ji, H. Chao, *Chem Comm* **2021**, *57*, 1790–1793.
[31] J.-X. Zhang, J.-W. Zhou, C.-F. Chan, T. C.-K. Lau, D. W. J. Kwong, H.-L. Tam, N.-K. Mak, K.-L. Wong, W.-K. Wong, *Bioconjug Chem* **2012**, *23*, 1623–1638.
[32] L. Wang, H. Yin, M. A. Jabed, M. Hetu, C. Wang, S. Monro, X. Zhu, S. Kilina, S. A. McFarland, W. Sun, *Inorg Chem* **2017**, *56*, 3245–3259.
[33] L. M. Lifshits, J. A. R. III, E. Ramasamy, R. P. Thummel, C. G. Cameron, S. A. McFarland, *J Photochem Photobiol* **2021**, *8*, 100067.
[34] R. Chen, Y. Huang, L. Wang, J. Zhou, Y. Tan, C. Peng, P. Yang, W. Peng, J. Li, Q. Gu, Y. Sheng, Y. Wang, G. Shao, Q. Zhang, Y. Sun, *Biomater Sci* **2021**, *9*, 2279–2294.
[35] J. B. Vermorken, R. Mesia, F. Rivera, E. Remenar, A. Kawecki, S. Rottey, J. Erfan, D. Zabolotnyy, H.-R. Kienzer, D. Cupissol, F. Peyrade, M. Benasso, I. Vynnychenko, D. de Raucourt, C. Bokemeyer, A. Schueler, N. Amellal, R. Hitt, *N Engl J Med* **2008**, *359*, 1116–1127.
[36] J. A. Bonner, P. M. Harari, J. Giralt, N. Azarnia, D. M. Shin, R. B. Cohen, C. U. Jones, R. Sur, D. Raben, J. Jassem, R. Ove, M. S. Kies, J. Baselga, H. Youssoufian, N. Amellal, E. K. Rowinsky, K. K. Ang, *N Engl J Med* **2006**, *354*, 567–578.
[37] M. Maalouf, G. Alphonse, A. Colliaux, M. Beuve, S. Trajkovic-Bodennec, P. Battiston-Montagne, I. Testard, O. Chapet, M. Bajard, G. Taucher-Scholz, C. Fournier, C. Rodriguez-Lafrasse, *Int J Radiat Oncol, Biol, Phys* **2009**, *74*, 200–209.
[38] Coliat, Ramolu, Jégu, Gaiddon, Jung, Pencreach, *Cancers (Basel)* **2019**, *11*, 1607.
[39] J.-Y. Zhou, W.-J. Wang, C.-Y. Zhang, Y.-Y. Ling, X.-J. Hong, Q. Su, W.-G. Li, Z.-W. Mao, B. Cheng, C.-P. Tan, T. Wu, *Biomaterials* **2022**, *289*, 121757.
[40] C. Tanielian, C. Wolff, M. Esch, *J Phys Chem* **1996**, *100*, 6555–6560.

TOC Graphics

A new Ru(II) cyclometalated complex activatable at 740 nm is reported as a photosensitizer for photodynamic therapy. Two ruthenium-cetuximab bioconjugates have been prepared to gain cancer cell specificity, but were found to be not phototoxic.

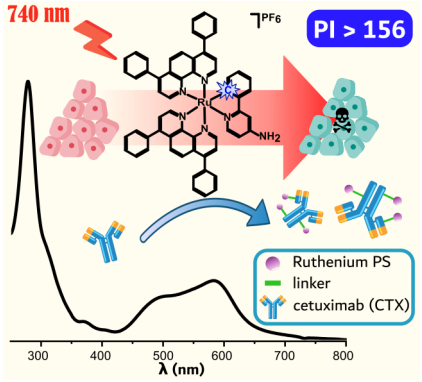

Twitter:
@marta.martinez.09, @Agandioso; @GasserGroup @ChimieParisTech @psl_univ